

Design of a High Performance Green-Mode PWM Controller IC with Smart Sensing Protection Circuits

¹Shen-Li Chen and ²Shih-Hua Hsu

^{1,2}Dept. of Electronic Engineering, National United University, MiaoLi City 36003, Taiwan

¹Tel.: +886-37381525, fax: +886-37362809

¹E-mail: jackchen@nuu.edu.tw

Received: 26 February 2014 /Accepted: 31 July 2014 /Published: 31 August 2014

Abstract: A design of high performance green-mode pulse-width-modulation (PWM) controller IC with smart sensing protection circuits for the application of lithium-ion battery charger (1.52 V ~ 7.5 V) is investigated in this paper. The protection circuits architecture of this system mainly bases on the lithium battery function and does for the system design standard of control circuit. In this work, the PWM controller will be with an automatic load sensing and judges the system operated in the operating mode or in the standby mode. Therefore, it reduces system's power dissipation effectively and achieves the saving power target. In the same time, many protection sensing circuits such as: (1) over current protection (OCP) and under current protection (UCP), (2) over voltage protection (OVP) and under voltage protection (UVP), (3) loading determination and short circuit protection (SCP), (4) over temperature protection (OTP), (5) VDD surge-spiking protection are included. Then, it has the characteristics of an effective monitoring the output loading and the harm prevention as a battery charging. Eventually, this green-mode pulse-width-modulation (PWM) controller IC will be that the operation voltage is 3.3 V, the operation frequency is 0.98 MHz, and the output current range is from 454 mA to 500 mA. Meanwhile, the output convert efficiency is range from 74.8 % to 91 %, the power dissipation efficiency in green-mode is 25 %, and the operation temperature range is between -20 °C ~ 114 °C.
Copyright © 2014 IFSA Publishing, S. L.

Keywords: Green-mode, Loading detection, Over current protection (OCP), Over temperature protection (OTP), Over voltage protection(OVP), Pulse-width-modulation (PWM), Short circuit protection (SCP), Under current protection (UCP), Under voltage protection (UVP).

1. Introduction

Because of the recent emergence of environmental awareness and green energy savings [1-6], effective power management in circuit design has become an important focus of development for the electronics industry. In the current consumer electronics market, portable electronic devices (e.g., cellphones) have become widely used in daily life, and the demands for portable electronic devices are now centered on the following characteristics:

1) Minimum size; 2) Light weight; 3) Extended operating time; and 4) Long standby time. Because of advancements in the process technology of integrated circuits (IC), control circuits and protection circuits using the existing switching mode power supply (SMPS) can now be incorporated onto chips, which have enabled the development of portable consumer electronics to emphasize lightness, thinness, and minimum size. To achieve light-weight and thin portable consumer electronics, all systems must be incorporated onto chips; to enable extended operating

time and standby time, power loss in the system chip should be mitigated. Power management control chips fulfill these demands by effectively managing chip conversion efficiency and reducing system power loss, thus achieving power savings and enhancing work effectiveness. However, commercial considerations (e.g., lightness and thinness) have resulted in a need to reduce battery size in overall product designs, which presents a challenge for designers regarding the provision of diverse functions, extended operating time, and prolonged standby time.

The majority of consumer electronics use lithium-ion batteries [7-12] because of the following advantages: 1) high capacitance density; 1.5- to 2.5-fold that of NiMH or NiCd batteries, 2) high voltage; a single lithium-ion battery cell can provide 3.6 V, which is substantially greater voltage than provided by NiMH and NiCd batteries (1.2 V), 3) strong electric charge reserve (i.e., low self-discharge); minimum power loss following long-term standby, 4) long battery life; up to 500 charge-discharge cycles with proper usage, 5) no memory effect; discharge is not required prior to charging.

The primary application of lithium-ion batteries is for cellphones, because the voltage range of lithium-ion batteries can range from 4.2 V when charged to 2.7 V after discharge, within which the majority of the discharge interval is maintained at approximately 3.6 V. Under normal operations, lithium-ion batteries discharge by converting chemical energy to electric energy through a positive chemical reaction. However, under certain circumstances such as charging, over discharge, or over current, chemical side reactions occur, thus affecting the properties and life of the battery. If such side reactions are exacerbated, a great amount of gas is produced within the battery, which rapidly increases pressure and may lead to an explosion. Therefore, a protective circuit is attached to all lithium-ion batteries to effectively protect and control charging and discharge. Furthermore, protective circuits will switch off the charging and discharge circuits under specific conditions to prevent battery damage during charging.

In the system design structure of common laptop computers, the primary power supply units include 1) A thin-film-transistor liquid-crystal display (TFT LCD) backlight power supply unit; 2) An AC-to-DC switching power supply unit; 3) A DC-to-DC

converter power supply unit; and 4) A lithium-ion battery unit. These units that require power supply also use a pulse-width modulation (PWM) controller [13-24] to manage and improve system conversion efficiency, thereby decreasing system power loss and saving electricity.

2. Green-mode PWM Control Circuits

The present study proposes a design that is highly efficient and contains a PWM controller (Fig. 1). The system design structure of this controller uses a lithium-ion battery charger, and the functions of the protective circuit in the lithium-ion battery are used for the system control design.

A voltage-current hybrid control model was employed in the system design structure of the PWM controller designed in the present study. Therefore, the entire control system uses different digital and analog circuits to determine the logic for various protection functions. The primary objective of this design is to access the voltage and amount of current when charging the lithium-ion battery for determining whether the controller is in an operation mode or green mode. TSMC 0.35 μm 2P4M 3.3 V CMOS process technology was used to design and analyze the various different circuits.

The control model provides protection for the output load side, such as 1) over voltage and under voltage protection, 2) over current and under current protection, 3) short circuit and overload protection, 4) over temperature protection (OTP), and 5) heavy and light load determination circuit. Thus, the control model can effectively monitor the output load side to prevent battery damage during charging.

Power surges may occur during system startup. The dead-time and soft-start circuit designed in the present study can be used to divide the voltage of power surges. Subsequently, normal feedback voltage (V_m) is outputted and then inputted into a voltage comparator and compared with a triangular wave voltage (V_p) for sampling. After the needed output duty cycle signal (V_{out}) of the power switch is obtained, the output cycle signal is determined by using a control circuit and driver circuit, and the power of the switching signal for the metal-oxide-semiconductor field-effect transistor (MOSFET) is amplified and outputted.

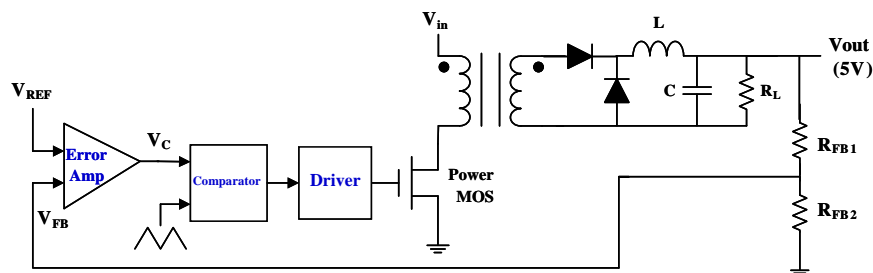


Fig. 1. Block and schematic diagram of a green-mode PWM controller IC.

3. Auto-sensing Protection Circuits in a PWM Controller IC

3.1. Current Limit Protection Circuit

Current limit protection is primarily used in for controlling the output load side of chargers, thereby preventing battery damage during charging. In addition, signals for current limit protection (I_{lim}) can be outputted to the control circuit for judgment. As shown in Fig. 2, the proposed circuit uses current limit protection. The circuit structure is primarily comprised of an over current protection circuit and under current protection circuit. In circuit design, current limit protection is used for maximum and minimum current limitation in load charge. Thus, according to regulations for lithium-ion battery charger design, the maximum and minimum working current is 5 V/600 mA and 5 V/50 mA, respectively. The circuit design specifications are detailed in Table 1.

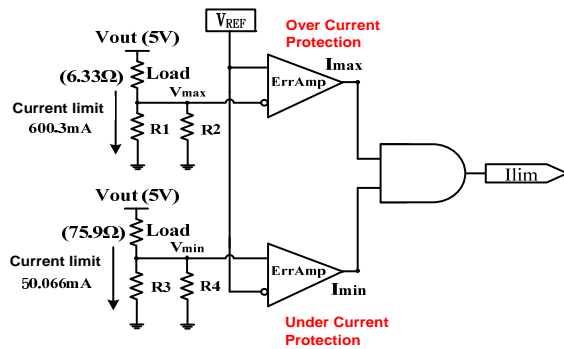


Fig. 2. Schematic diagram of the current limit circuit.

Table 1. Specifications of the current limit protection circuit.

V_{out}	Current	600.3 mA	50.066 mA
	$5\text{ V } (V_{typ})$	Loading resistance	6.33 Ω

3.1.1. Over Current Protection Circuit

The first circuit shown in Fig. 2 is an over current protection circuit. The circuit is connected beneath the load component through small resistance (R_1 and R_2), thereby accessing the current during load charge. Subsequently, the current signal is converted into a voltage (V_{max}), which is then inputted into an error amplifier (ErrAmp) and compared against a reference voltage (V_{REF}) to acquire voltage difference. Finally, the outputted voltage signal (I_{max}) is inputted into the logic circuit and used for determination with the under current protection signal (I_{min}). Over current protection is primarily used

as a limit for maximum power current during load component charge; therefore, the maximum working current was set as 5 V/600 mA.

3.1.2. Under Current Protection Circuit

The second circuit shown in Fig. 2 is a under current protection circuit. The circuit is connected beneath the load component through small resistance (R_3 and R_4), thereby accessing the current during load charge. Subsequently, the current signal is converted into a voltage (V_{min}), which is then inputted into an ErrAmp and compared against a reference voltage (V_{REF}) to acquire voltage difference. Finally, the outputted voltage signal (I_{min}) is inputted into the logic circuit and used for determination with the current protection signal (I_{max}). Under current protection is primarily used as a current limit for short circuiting during load component charge; therefore, the minimum working current was set as 5 V/50 mA.

3.2. Voltage Limit Protection Circuit

Voltage limit protection is primarily used in for controlling the output load side of chargers, thereby preventing battery damage during charging. In addition, signals for voltage limit protection (V_{lim}) can be outputted to the control circuit and system loop for judgment.

The circuit shown in Fig. 3 is a voltage protection limit circuit. The circuit structure is primarily comprised of an over current protection circuit and under current protection circuit. In circuit design, voltage limit protection is used for maximum and minimum voltage supply limitation during load charge. Thus, according to regulations for lithium-ion battery charger design, the maximum and minimum voltage is 7.5 V and 1.52 V, respectively. The circuit design specifications are detailed in Table 2.

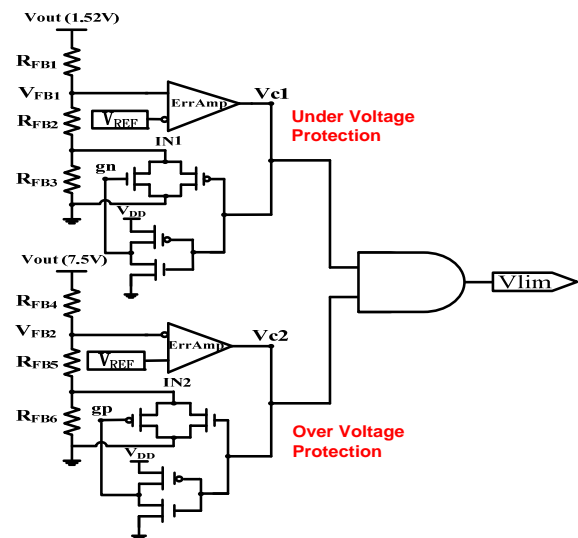


Fig. 3. Schematic diagram of the voltage limit circuit.

Table 2. Specifications of the voltage and current limit protection circuits.

V _{out}	Current	600.3 mA	50.066 mA
	Loading resistance	10.494 Ω	125.84 Ω
7.5 V (V _{max})		10.494 Ω	125.84 Ω
5 V (V _{typ})		6.33 Ω	75.9 Ω
1.52 V (V _{min})		0.534 Ω	6.377 Ω

3.2.1. Under Voltage Protection Circuit

The circuit shown in Fig. 4 is a under voltage protection circuit. The circuit primarily outputs feedback resistance (R_{FB1}, R_{FB2}, and R_{FB3}) into the output voltage (V_{out}), thereby accessing the feedback voltage (V_{FB1}). Subsequently, the feedback voltage is inputted into an ErrAmp and compared against a reference voltage (V_{REF}). Finally, the outputted voltage signal (Vc1) is inputted into the logic circuit and used for determination with the over voltage protection signal (Vc2).

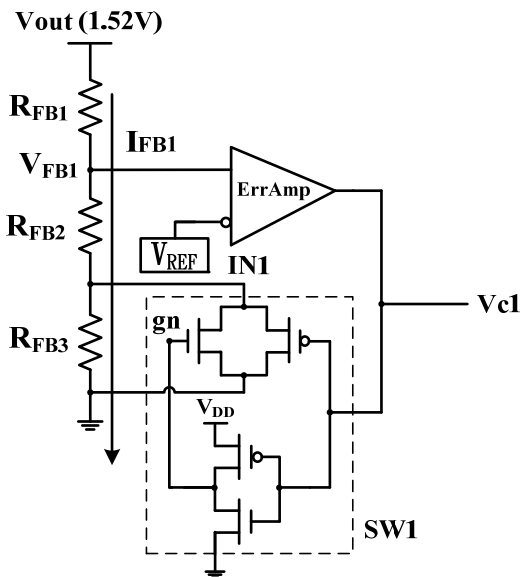


Fig. 4. Schematic diagram of the under voltage protection circuit.

Fig. 5 shows the basic circuit design of a under voltage protection circuit, which primarily designed based on the minimum working current (I_{lim} (min)) and minimum work load (6.33 Ω) of the current limit protection circuit. The following formula was used to obtain the minimum supply voltage (V_{out} (min)). The circuit structure of under voltage protection circuits primarily uses a latch to limit the minimum working voltage when operating the PWM controller; thus, the latch for under voltage protection was set as 1.52 V.

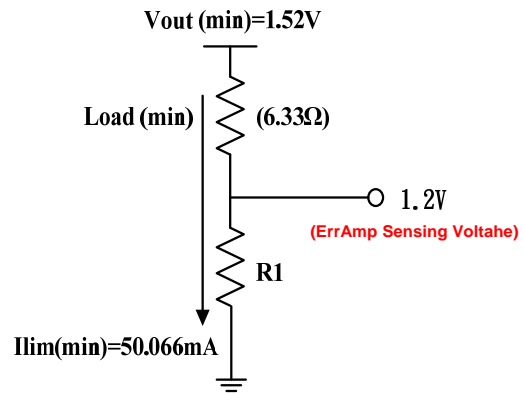


Fig. 5. Main architecture of the under voltage protection circuit.

3.2.2. Over Voltage Protection Circuit

The circuit operation principle of the over voltage protection circuit shown in Fig. 6 is detailed as follows: When the output voltage (V_{out}) is 7.5 V and the feedback voltage (V_{FB2}) is lower than the reference voltage (V_{REF}), the voltage signal is outputted as a Hi level, and the switch (SW2) is conducted. Subsequently, the feedback voltage (V_{FB2}) is reduced, remaining less than the reference voltage (V_{REF}). Thus, the ErrAmp output is converted to a Hi level, and the switch (SW2) is only switched off when the output voltage (V_{out}) exceeds 7.5 V. Subsequently, the voltage signal (Vc2) is outputted at a under level for over voltage protection. Over voltage protection is primarily used as a limit for maximum power voltage during load component charge; therefore, the maximum supply voltage was set as 7.5 V, which is 1.5-fold the normal output voltage (V_{out}).

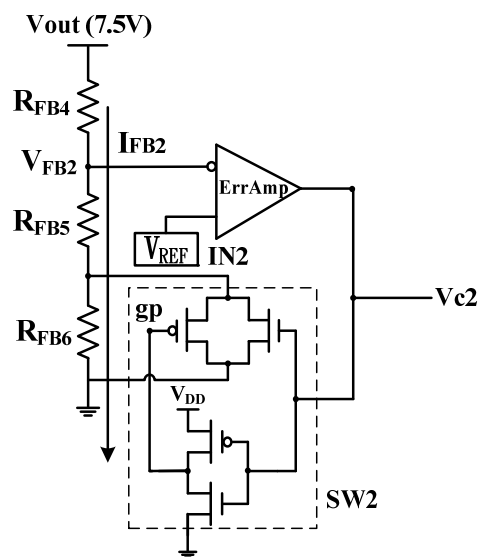


Fig. 6. Schematic diagram of the over voltage protection circuit.

3.3. Loading Detected Circuit

Heavy and light load determination circuits are primarily used for controlling the power usage on the output load side of chargers. Automatic system switches are conducted according to load usage. Thus, system power loss is effectively decreased during operation mode and green mode, thereby saving electricity. The circuit shown in Fig. 7 is a heavy and light load determination circuit.

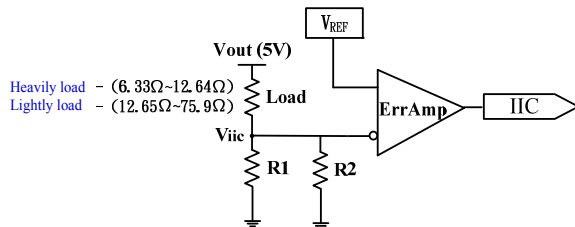


Fig. 7. Schematic diagram of the loading sensing circuit.

The circuit is connected beneath the load component through small resistance (R1 and R2), which facilitates the reading of different currents and determination regarding whether the system is in

operating mode or green mode. The detailed design specifications are shown in Table 3.

Table 3. Specifications of the loading sensing circuit.

Current V_{out}	600.3 mA	300.6 mA	300.4 mA	50.066 mA
	Loading resistance	Loading resistance	Loading resistance	Loading resistance
5 V (V_{typ})	6.33 Ω	12.64 Ω	12.65 Ω	75.9 Ω
Loading sensing	Heavy load		Light load	

3.4. Over Temperature Protection Circuit

In system circuit design, OTP is primarily used for controlling heat increase in the output load side of operating chargers. Circuit latching can be conducted according to default temperature protection conditions. The circuit design of the bandgap voltage reference (BGR) OTP circuit shown in Fig. 8 primarily uses the properties of BGR to equal the bipolar transistor (D1) into a diode form; hence, temperature changes during load charge can be accessed. The design specifications of the circuit are detailed in Table 4.

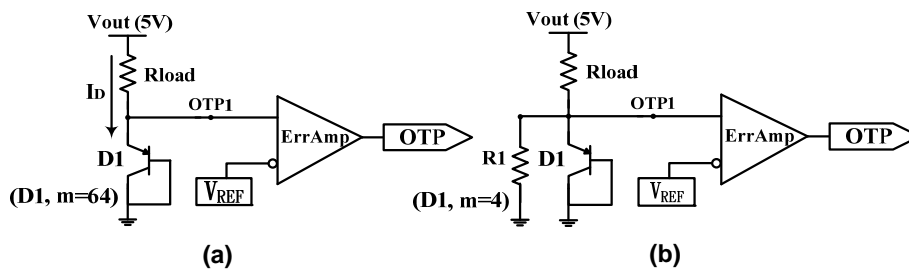


Fig. 8. Schematic diagram of the over temperature protection circuit of BGR-type as (a) loading 600.3 mA; (b) loading 50.066 mA.

Table 4. Specifications of the over temperature protection circuit of BGR-type.

V_{out} Loading current	7.5 V	5 V	1.52 V
	Loading resistance	Loading resistance	Loading resistance
600.3 mA	10.494 Ω	6.33 Ω	0.534 Ω
OTP	118 $^{\circ}\text{C}$	118 $^{\circ}\text{C}$	118 $^{\circ}\text{C}$
50.066 mA	125.84 Ω	75.9 Ω	6.377 Ω
OTP	118 $^{\circ}\text{C}$	118 $^{\circ}\text{C}$	120 $^{\circ}\text{C}$

3.5. Dead-time and Soft-start Circuit

The dead-time and soft-start circuit shown in Fig. 9 is primarily used for absorbing power surges that occur during system startup. Thus, the transmission of erroneous output signals to the power MOSFET switch are prevented, thereby avoiding

malfunction. Power surge during system startup is a temporary phenomenon. The voltage of power surges are divided through the proposed dead-time and soft-start circuit, and surge duration is extended. Thus, normal output feedback voltage (V_m) is obtained. The details of compensated capacitance are shown in Table 5.

Circuit settling time is extended when prolonged power surges occur, during which the use of compensated capacitance will further lengthened. However, the precise point in time of power surge occurrence is unpredictable. The results of the transient analysis indicate that power surges do not cause circuit output malfunctions, but increase settling time. Therefore, when designing the proposed protection circuit, capacitance was not added as compensation. Consequently, the present study provides an explanation regarding circuit function as reference for circuit compensation during

power surges. In general, capacitance compensation for power surges is achieved by accessing the 25th to 75th cycle of the system output duty cycles, thereby achieving power surge compensation during system soft-startup.

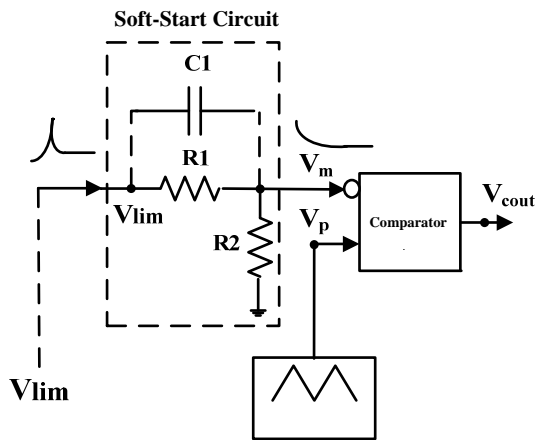


Fig. 9. Schematic diagram of the soft-start circuit.

Table 5. Specifications of the spiking compensated capacitance of VDD source.

VDD transient noise	Compensated capacitance (C1)	Settling Time in V _{cout}
5 V	–	0.995 μs
5 V	1 pF	0.996 μs
5 V	10 pF	0.994 μs
5 V	100 pF	4.56 μs
5 V	200 pF	9.19 μs

3.6. Whole Control Circuits

The overall control circuit is primarily used for the logic determination of the output protection functions for various protection circuits. The determination signal can be outputted to the next

level driver circuit for driving power MOSFET switch control. The control circuit shown in Fig. 10 uses a digital logic circuit for the logic determination of the following protection functions: 1) Loop control signals (V_{cout}), 2) Current limit protection (I_{lim}), voltage limit protection (V_{lim}), 3) OTP, 4) Heavy and light load determination control signals (I_{lc}), and 5) System reset control signals. Thus, the count of the determination signals can be outputted to the next driver circuit for control.

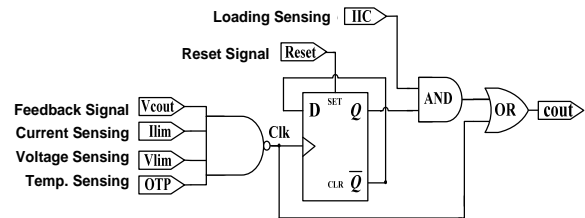


Fig. 10. Block diagram of the whole controller circuits.

4. Whole System Circuit

The circuit shown in Fig. 11 possesses a comprehensive green-mode PWM controller system structure. The circuit comprises a voltage limit protection circuit, current limit protection circuit, heavy and light load determination circuit, OTP circuit, dead-time and soft-start circuit, control circuit, and driver circuit. The operation of the OTP circuit is used as an example. The output remains at a Hi level when the OTP circuit is at a temperature between 100 °C and 113 °C. However, when temperatures exceed 114 °C, the output is converted to a low level (i.e., the OTP circuit is activated), as shown in Fig. 12. The system development specifications of the green-mode PWM controller are detailed in Table 6.

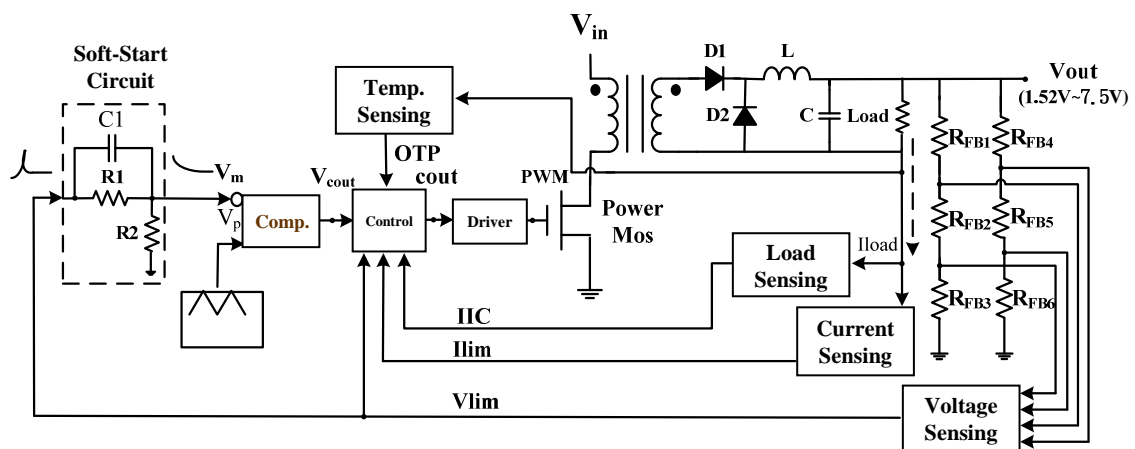


Fig. 11. Block and schematic diagram of the whole PWM controller circuits.

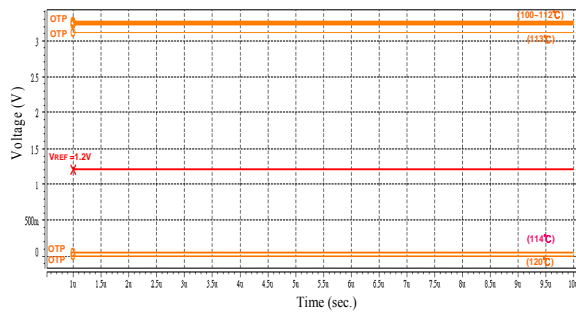


Fig. 12. Output voltage responds during the OTP circuit function working (114 °C).

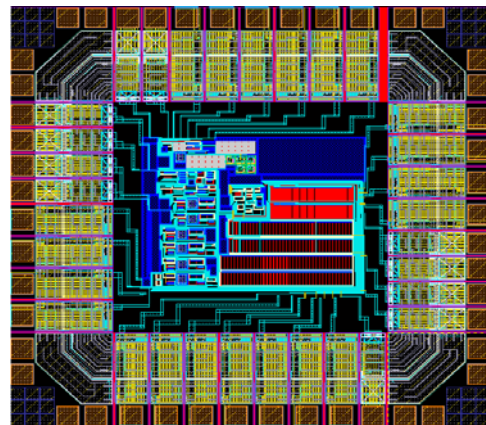
Table 6. Specifications of the green-mode PWM controller IC.

Operating Conditions			
Operation Voltage (VDD)	3.3 V		
Operation frequency	0.98 MHz		
Output Voltage (V_{out})	3 V		
Output Current (I_{out})	500 mA		
Resistance: Power MOS	6 Ω		
Output Convert Efficiency (Power)	91 %		
Dissipation Efficiency (Green Mode)	25 %		
Reference Voltage	1.2 V		
Operation Temperature Range	-20 °C~114 °C		
Protection Conditions	Min	Typ	Max
Load Working Range	0.534 Ω	-	125.84 Ω
Over Voltage Protection (OVP)	-	5 V	7.5 V
Under Voltage Protection (UVP)	1.52 V	5 V	-
Over Current Protection (OCP)	-	-	600.3 mA
Under Current Protection (UCP)	50.066mA	-	-
Short Circuit Protection (SCP)	< 1.52 V	-	-
	< 50.066 mA	-	-
Over Power Protection (OPP)	-	-	4.5 W
Heavy Load Determination	-	300.6 mA	600.3 mA
Light Load Determination	50.066 mA	300.4 mA	-
Over Temperature Protection (OTP)	-	-	114 °C

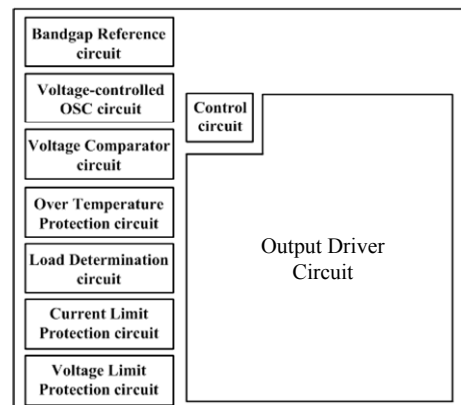
The circuit layout shown in Fig. 13 is that of a green-mode PWM controller. The system circuit of the controller was designed based on the process technology of TSMC 0.35 μm 2P4M 3.3 V CMOS. The final circuit layout area was 1.71 mm \times 1.633 mm.

The PWM controller comprises of digital and analog circuits; therefore, the bandgap reference and voltage-controlled oscillation circuit (OSC), which are easily subjected to noise, were placed on the top left of the chip during system circuit layout. In addition, guard rings were used for grounding to prevent circuit noise interference. Different power supply combinations (VDD1 and VSS1; VDD2 and VSS2) are used to provide an independent and stable power supply.

The output stage is subjected to long-term operations under high-speed bulk current changes. To prevent high-temperature noise from influencing other digital and analogue circuits during system switch, the circuit was placed at the bottom right of the chip during layout. Guard rings were used for grounding to prevent circuit noise interference. Independent power supply (VDD4 and VSS4) is used to provide a stable power source.



(a)



(b)

Fig. 13. (a) Layout top-view; (b) block diagram of green-mode PWM controller IC.

5. Conclusion

The objective of this work is to develop a detailed system circuit and smart sensing protection design for a green-mode PWM controller. In addition, HSpice

AC, DC, and transient simulation analyses are conducted on the properties of the proposed system circuit and protection circuit: error amplifier circuit, bandgap reference voltage circuit, voltage comparison circuit, voltage-controlled OSC, current limit protection circuit, voltage limit protection circuit, heavy and light load circuit, OTP circuit, control circuit, and output circuit. Subsequently, specific regulations are employed to design the system for the green-mode PWM controller.

The TSMC 0.35 μm 2P4M 3.3 V CMOS process technique was employed in the present study. The system design specifications are detailed as follows: 3.3 V operating voltage, 0.98 MHz operating frequency, output voltage range between 2.72 V and 3 V, output current range between 454 mA and 500 mA, output conversion efficiency range between 74.8 % and 91 %, output conversion efficiency at 25% under green mode, and operating temperature range between -20 °C and 114 °C. The specifications for the automatic detecting protection design of the controller are detailed as follows: over voltage protection range between 5 V and 7.5 V, under voltage protection range between 1.52 V and 5 V, over current protection= 600.3 mA, under current protection= 50.066 mA, short circuit protection < 1.52 V, over circuit protection= 4.5 W, heavy load determination range between 300.6 mA and 600.3 mA, light load determination range between 50.066-mA and 300.4 mA, and OTP protection= 114 °C. Therefore, the proposed circuit is considered a smart green-mode PWM controller.

Acknowledgements

In this work, authors would like to thank the National Chip Implementation Center in Taiwan for providing the process information platform.

References

- [1]. Shun-Chung Wang, Chi-Feng Su, Chien-Hung Liu, High power factor electronic ballast with intelligent energy saving control for ultraviolet lamps drive, in *Proceedings of the Industry Applications Conference*, 2005, pp. 2958 - 2964.
- [2]. Hung-Da Hsu, Tsorng-Juu Liang, Bin-Da Liu, Kai-Hui Chen. Design of a green mode PWM control IC, *IEEE Asia Pacific Conference on Circuits and Systems*, 2008, pp. 1876-1879.
- [3]. Jiana Lou, Xiaobo Wu, Hai Chen, Xiaolang Yan, Design of High Efficiency Green Mode SMPS Regulator, in *Proceedings of the 4th IEEE International Conference on Circuits and Systems for Communications*, 2008, pp. 564-567.
- [4]. Zheng Chen, Dongsheng Ma, A 10 MHz 92.1%-efficiency green-mode automatic reconfigurable switching converter with adaptively compensated single-bound hysteresis control, *IEEE International Solid-State Circuits Conference*, 2010, pp. 204-205.
- [5]. Zheng Chen, Dongsheng Ma. A 10-MHz Green-Mode Automatic Reconfigurable Switching Converter for DVS-Enabled VLSI Systems, *IEEE Journal of Solid-State Circuits*, Vol. 46, Issue 6, 2011, pp. 1464-1477.
- [6]. Khalid Raza, V. K. Patle, Sandeep Arya, A Review on Green Computing for Eco-Friendly and Sustainable IT, *Journal of Computational Intelligence and Electronic Systems*, Vol. 1, Issue 1, 2012, pp. 3-16.
- [7]. A. M. Rahimi, A lithium-ion battery charger for charging up to eight cells, *IEEE Conference Vehicle Power and Propulsion*, 2005, pp. 131-136.
- [8]. M. F. M. Elias, K. M. Nor, A. K. Arof, Design of Smart Charger for Series Lithium-Ion Batteries, in *Proceedings of the International Conference on Power Electronics and Drives Systems*, 2005, pp. 1485-1490.
- [9]. Min Chen, G. A. Rincon-Mora, Accurate, Compact, and Power-Efficient Li-Ion Batter Charger Circuit, *IEEE Transactions on Circuits and Systems II: Express Briefs*, Vol. 53, Issue 11, 2006, pp. 1180-1184.
- [10]. Lan Dai, Ke-Qing Ning, Yan-Feng Jiang, Design of a multi-mode and high-stability linear charger for Lithium-ion batteries, in *Proceedings of the 10th IEEE International Conference on Solid-State and Integrated Circuit Technology (ICSICT)*, 2010, pp. 345-347.
- [11]. A. Al-Refai, R. Abou Sleiman, O. A. Rawashdeh, A programmable charger for monitoring and control of multi-cell lithium-ion batteries, *IEEE National Aerospace and Electronics Conference (NAECON)*, 2012, pp. 68-74.
- [12]. Faa-Jeng Lin, Ming-Shi Huang, Po-Yi Yeh, Han-Chang Tsai, Chi-Hsuan Kuan, DSP-Based Probabilistic Fuzzy Neural Network Control for Li-Ion Battery Charger, *IEEE Transactions on Power Electronics*, Vol. 27, Issue 8, 2012, pp. 3782-3794.
- [13]. Q. M. Li, A low-cost configurable PWM controller using programmable system-on-chip, in *Proceedings of the IEEE 34th Annual Power Electronics Specialist Conference*, 2003, pp. 1169-1174.
- [14]. Zhaoyong Zhou, Tiejai Li, T. Takahashi, E. Ho, Design of a universal space vector PWM controller based on FPGA, in *Proceedings of the 19th Annual IEEE Applied Power Electronics Conference and Exposition*, 2004, pp. 1698-1702.
- [15]. R. K. Pongiannan, N. Yadaiah, FPGA based Space Vector PWM Control IC for Three Phase Induction Motor Drive, in *Proceedings of the IEEE International Conference on Industrial Technology*, 2006, pp. 2061-2066.
- [16]. Chang-Gyu Yoo, Woo-Cheol Lee, Kyuchan Lee, Inyoung Suh, Current Mode PWM Controller for a 42 V / 14 V bidirectional DC/DC Converter, in *Proceedings of the 37th IEEE Power Electronics Specialists Conference*, 2006, pp. 1-6.
- [17]. Z. Lukic, Christopher Blake, S. C. Huerta, A. Prodic, Universal and Fault-Tolerant Multiphase Digital PWM Controller IC for High-Frequency DC-DC Converters, in *Proceedings of the Twenty Second Annual IEEE Applied Power Electronics Conference*, 2007, pp. 42-47.
- [18]. Li-Jen Liu, Yeong-Chau Kuo, Wen-Chieh Cheng, Analog PWM and Digital PWM Controller IC for DC/DC Converters, in *Proceedings of the 4th International Conference on Innovative Computing*,

- Information and Control (ICICIC), 2009, pp. 904-907.
- [19]. Jiaying Lu, Xiaobo Wu, A novel multiple modes PWM controller for LEDs, in *Proceedings of the IEEE International Symposium on Circuits and Systems*, 2009, pp. 1767-1770.
- [20]. Jiaying Lu, Xiaobo Wu, A PWM Controller IC for LED Driver Used to Multiple DC-DC Topologies, in *Proceedings of the Asia-Pacific Power and Energy Engineering Conference*, 2009, pp. 1-4.
- [21]. Lingling Dong, Yidie Ye, Lenian He, A Novel PWM Controller IC for LED Driver with Frequency Spread, in *Proceedings of the Asia-Pacific Power and Energy Engineering Conference*, 2010, pp. 1-4.
- [22]. Seong Wha Hong, Hong Jin Kim, Joon-Sung Park, Young Gun Pu, Jeongin Cheon, Dae-Hoon Han, Kang-Yoon Lee, Secondary-Side LLC Resonant Controller IC With Dynamic PWM Dimming and Dual-Slope Clock Generator for LED Backlight Units, *IEEE Transactions on Power Electronics*, Vol. 26, Issue 11, 2011, pp. 3410-3422.
- [23]. Yun She, Output Feedback Control of Electronic Throttle Valve, *Journal of Mechatronics*, Vol. 1, Issue 1, 2012, pp. 3-11.
- [24]. Young Hwan Lho, Yeu Sung Hwang, Sang Yong Lee, A study on radiation effects on PWM-IC controller of DC/DC power buck converter, in *Proceedings of the 13th International Conference on Control, Automation and Systems (ICCAS)*, 2013, pp. 1754-1757.

2014 Copyright ©, International Frequency Sensor Association (IFSA) Publishing, S. L. All rights reserved.
(<http://www.sensorsportal.com>)

Universal Sensors and Transducers Interface (USTI)

for any sensors and transducers with frequency, period, duty-cycle, time interval, PWM, phase-shift, pulse number output



The image shows three USTI integrated circuits: a large DIP package, a smaller QFP package, and a tiny MLF package. To the left, there are five white icons on a red background: a square wave, a variable resistor, a variable capacitor, a diamond-shaped bridge circuit, and a gear.

- * Input frequency range: 0.05 Hz ... 9 MHz (144 MHz)
- * Selectable and constant relative error: 1 ... 0.0005 % for all frequency range
- * Scalable resolution
- * Non-redundant conversion time
- * RS232, SPI, I2C interfaces
- * Rotational speed, *rpm*
- * Cx, 50 pF to 100 μ F
- * Rx, 10 Ω to 10 M Ω
- * Pt100, Pt1000, Pt5000, Cu, Ni
- * Resistive Bridges
- * PDIP, TQFP, MLF packages

Just make it easy !

<http://www.techassist2010.com/> info@techassist2010.com